Tsakona et al., Cell Dev Biol 2018, 7:2
DOI: 10.4172/2168-9296.1000198

Cell & Developmental Biology

Research Article Open Access

Identification with SILAC Proteomics of Novel Short Linear Motifs in Demethylase Enzymes Regulated During Myoblast Differentiation

Dimitra Tsakona[1], Panagiota A. Galliou[2] and Nikolaos A. Papanikolaou[2]*

[1]*Department of Biology, School of Natural Sciences, Aristotle University of Thessaloniki, Macedonia, Greece*
[2]*Laboratory of Biological Chemistry, Department of Medicine, Section of Biological Sciences and Preventive Medicine, School of Health Sciences, Aristotle University of Thessaloniki, Macedonia, Thessaloniki, Greece*

Abstract

Methylation and demethylation of Lysine and Arginine on proteins is quantitatively an extensive and functionally a significant post-translational modification yet there is a dearth of information at a functional systems level. Using SILAC proteomics and high resolution mass spectrometry we have identified eight demethylase and two methylase proteins whose levels are regulated during myogenic differentiation in a mouse myoblast-to-myocyte model. Using the general methylation inhibitor adenosine dialdehyde (AdOX) we established that methylation is required for differentiation. Whole proteome analysis revealed that 1134 out of 4600 proteins identified were differentially expressed, of which 488 were up-regulated and 646 down-regulated. Of these, two were methylases and eight were demethylases. Notably, five of the eight enzymes demethylate Lysine 9 on histone 3 (H3K9) whereas two also demethylate H3K4. Lastly, we have identified short linear motifs (SliMs) in the demethylase enzymes that are enriched in differentiation. We briefly discuss the significance of our findings within a developmental/epigenomics framework.

Keywords: Short linear motifs; Differentiation; Myoblast; Myocyte; SILAC proteomics; Demethylase; Methylase

Abbreviations: AdOX: Adenosine Dialdehyde; DMEM: Dulbecco Modified Eagle's Medium; FBS: Fetal Bovine Serum; LC: Liquid Chromatography; MS: Mass Spectrometry; SILAC: Stable Isotope Labeling with Amino acids in Cell culture; SLiM: Short Linear Motif

Introduction

Skeletal muscle is generated from the multi-stage differentiation of myoblast precursors of somite mesenchymal origin in late embryogenesis and comprises nearly 40% of total body mass in humans [1]. Myoblasts are skeletal mononuclear myocytes that are committed to the myogenic lineage but also are capable of proliferation in cell culture. During differentiation, myoblasts elongate and fuse with each other forming multinucleated, terminally differentiated myocytes, capable of contraction [2,3]. Induction of myocyte differentiation is initiated by the successive activation of signaling pathways that cooperate in the inhibition of proliferation and in the induction of differentiation via expression of several muscle differentiation-specific transcription factors, such as the basic-helix-loop muscle regulatory Myf5 protein, which is expressed first in the developing embryo, followed by MyoD, myogenin and MRF5 [4,5]. At the molecular level the most important genes that control myogenesis are the transcription factor Myogenic differentiation antigen, MyoD, and the Retinoblastoma protein, Rb [6,7]. The molecular agents above also coordinate cell cycle progression with induction of gene programs that commit cells to differentiation. Specifically, the activated Rb protein induces cell cycle arrest along with the CDK inhibitors WAF1/p21 and p27 and myogenin. These events are followed by differentiation-specific expression of markers such as troponin T. Several pathways regulate differentiation of C2C12 mouse myoblast cells. For example, the Notch pathway inhibits terminal differentiation through activation of expression of the transcriptional regulator human C promoter Binding Factor (CBF1) [8,9]. In contrast, the histone acetyltransferase PCAF enhances the MyoD-mediated transcription and myogenic differentiation, presumably through complex formation with MyoD, leading to activation of expression of WAF1/p21 [10-12]. Also, ERK6, a member of the MAPK family of mitogen-activated Serine/Threonine protein kinases as well as p38 activator MAP kinase (MKK3) have been implicated in C2C12 cell myogenic differentiation [13].

Although the role of individual signaling pathways in muscle differentiation has been studied, few global studies have addressed the role of post-translational modifications during this process [14]. Mouse myoblast C2C12 cells are a suitable experimental model to dissect on a proteomic scale differences in the levels of proteins between proliferating myoblasts and differentiated myocytes [15,16]. We therefore undertook a SILAC-based quantitative profiling of proteome changes in proliferating myoblasts and differentiated myocytes using high resolution tandem mass spectrometry analysis [17,18] and generated a comprehensive list of proteins whose levels change significantly between proliferating myoblasts and differentiated myocyte cells [15]. Whole proteome changes revealed that the levels of at least eight demethylase and two methylase enzymes are significantly altered suggesting that they might play key roles in the differentiation process.

Materials and Methods

Reagents

SILAC amino acids, L-lysine (13C615N2, Cat# CNLM-291-632) and L-Arginine (13C615N4, Cat# CNLM-539-H-1) were purchased from Cambridge Isotope Laboratories Inc, MA. TPCK-treated trypsin was from Worthington Biochemical Corp (Lakewood, NJ). Regular DMEM and DMEM deficient of L-Lysine or L-Arginine were from Thermo Scientific. Fetal Bovine Serum (FBS), antibiotics and phosphate buffered saline (PBS, pH 7.4) were obtained from Invitrogen (Carlsbad, CA). Iodoacetamide and DL-Dithiothreitol were from Sigma. Adenosine dialdehyde, AdOX, was from Sigma-Aldrich, USA.

***Corresponding author:** Nikolaos A. Papanikolaou, Ph.D, Laboratory of Biological Chemistry, Department of Medicine, School of Health Sciences, Aristotle University of Thessaloniki, Panepistimioupolis, Bldg 16a, 3rd Floor, Thessaloniki, Macedonia, 54124 Greece, Tel: (30)2310999003; Fax: (30)2310999002; E-mail: papanikn@med.auth.gr

Received August 10, 2018; **Accepted** December 17, 2018; **Published** December 24, 2018

Citation: Tsakona D, Galliou PA, Papanikolaou NA (2018) Identification with SILAC Proteomics of Novel Short Linear Motifs in Demethylase Enzymes Regulated During Myoblast Differentiation. Cell Dev Biol 7: 198. doi:10.4172/2168-9296.1000198

Cell culture, SILAC labeling and Microscopy

Mouse muscle myoblast cells C2C12 were obtained from American Tissue and Cell Culture (ATCC, VA) and maintained in DMEM supplemented with 20% FBS, penicillin/streptomycin at 37°C and 5% CO_2. For differentiation, cells were grown to confluence in 15 cm dishes (Corning, NY), then switched to DMEM with 2% FBS and allowed to differentiate for five days. Proliferating C2C12 were labeled with SILAC amino acids as described previously [15]. Briefly, C2C12 cells were cultured in DMEM supplemented with 20% FBS and SILAC amino acids L-lysine ($^{13}C_6{}^{15}N_2$) and L-Arginine ($^{13}C_6{}^{15}N_4$). After five doublings, it was confirmed that all proliferating C2C12 cells were fully labeled. SILAC-labeled proliferating C2C12 or non-labeled differentiated C2C12 cell extracts were separately prepared according to the manufacturer's instructions (Thermo Scientific, Figure 1). Microscopy was performed with a Nikon microscope using a DXM1200F camera and fields were photographed at 40X or 100X. Typically, cell culture dishes at days 1, 3 and 5 were removed and aseptically examined for differentiation and cell death and then returned to the culture hood.

Peptide sample preparation for whole cell proteomic analysis

Three hundred micrograms of proteins (total 600 µg) each from proliferating C2C12 (SILAC-labeled) and differentiated C2C12 (non-labeled) were mixed. Proteins were reduced with 5 mM dithiothreitol for 30 min at room temperature, alkylated with 10 mM Iodoacetamide for 20 min in the dark, diluted with 20 mM HEPES pH 8.0 to a final concentration of 1.5 M urea and digested with sequencing grade trypsin (Promega) at 1:30 w/w of enzyme to protein ratio overnight at room temperature. Digested peptides were desalted using Sep-Pak light cartridges and fractionated into 96 fractions by basic RPLC chromatography. These 96 fractions were concatenated into 12 fractions prior to drying by speed vacuum. Three independent biological replicate experiments were performed and independent extract samples were prepared prior to peptide purification.

Liquid chromatography tandem mass spectrometry

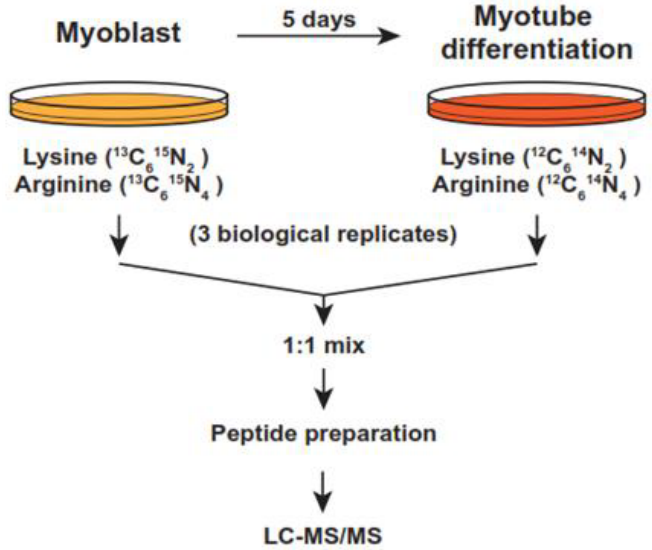

Figure 1: Heavy amino acid SILAC strategy method used to identify the proteins whose levels are regulated during myoblast differentiation. For details see Materials and Methods. Three independent biological replicates were performed.

LC-MS/MS analysis of the three biological replicates, each from 12 fractions, was carried out on an LTQ Orbitrap Elite mass spectrometer (Thermo Scientific, Bremen, Germany) interfaced with Easy nLC II (Thermo Scientific, Bremen, Germany). The peptides were loaded on an enrichment column (75 µm×2 cm) packed in-house (particle size 3µm; ReproSil-Pur 100 Basic C18) and separated on a ReproSil-Pur 100 Basic C18 analytical column (75µm×10 cm; particle size 2.3 µm) using a linear gradient of 7% to 45% solvent B (0.1% formic acid in 90% acetonitrile) for 100 minutes with a total run time of 120 minutes. The mass spectrometer was operated in the FT-FT mode. Survey scans and data-dependent MS/MS spectra were acquired at a resolving power of 120,000 and 30,000, respectively. Twenty most intense precursor ions from a survey scan within an m/z range of 350 to 1,800 were isolated with a 2 Dalton window and fragmented by HCD with 40% normalized collision energy. A dynamic exclusion of 45 secs was used with a 7 ppm window. Internal calibration was carried out using lock mass option (m/z 445.1200025) from ambient air.

Mass spectrometry data analysis

The proteome Discoverer platform 2.0 suite (Thermo Fisher Scientific, Bremen, Germany) was used for peak list generation and database searches. A precursor mass range of 350-8000 Da and signal to noise ratio of 1.5 were the criteria used for generating peak lists. The SEQUEST search algorithm was used for database searches with NCBI RefSeq 79 as a reference database (containing common contaminants). The oxidation of Methionine and SILAC 2-plex (13C615N L-lysine and 13C615N4 L-Arginine) were used as dynamic modifications. The Carbamidomethylation of Cysteine residue was used as a static modification. A maximum of one missed cleavage was allowed for tryptic peptides. Mass error windows of 5 ppm and 0.02 Da were allowed for precursors and fragments, respectively. A decoy database was used to calculate the False Discovery Rate (FDR) with a cut-off of 1%.

Short Linear Motif (SLiM) Identification

SliMs were identified using the default settings on the MEME suite. FASTAs of eight demethylases and two methylases were extracted from the UNIProt database and analyzed for the presence of SliMs.

Gene Ontology (GO) analysis

Analysis of genes enriched in the up- or downregulated lists was performed on-web on the PANTHER site (http://pantherdb.org/) using default settings. For overrepresentation we employed PANTHER, version 13.1 Released 2018-02-03 using the nnotation data set "Reactome Gene Ontology Complete, version 65" 2018-06-12 Release. The Reference set was all mouse genes in the database. Statistical analysis was with the Fisher exact test using the Bonferroni correction.

Demethylase network reconstruction and analysis

In order to reconstruct a demethylase network for differentiating C2C12 mouse myoblast cells, we used the eight demethylase enzymes, found to undergo significant changes in their levels during myoblast differentiation, as queries and extracted their experimentally verified ($E \geq 0.7$) interactions from the STRING (https://string-db.org/) database using the following settings: First level (shell) of interactions: 20 interactors, second level of interactors: 100 interactors. A total of 137 interactors for the 8 demethylase enzymes were retrieved ($E \geq 0.7$), having 1848 edges, with an average node degree of 27.2, average local clustering equal to 0.715 and a p enrichment <1.0e-16. Binary relationships were subsequently analyzed with Cytoscape (https://cytoscape.org/) and clustered around the top significant ($p \leq 0.001$) functional GO clusters with the MCODE subroutine and verified

with the GeneOntology (PANTHER) online set of algorithms (http://geneontology.org/page/go-enrichment-analysis) shown in Figures 4A and B. The cytoHubba algorithm was used to extract the top ten bottlenecks (Figure 6A) and computed shortest paths Figure 6B).

Result and Discussion

The goal of this study was to identify protein families that are regulated in the C2C12 mouse cell differentiation model employing the strategy shown in Figure 1 using SILAC proteomics with heavy, non-radioactive amino acids, as described in Materials and Methods [15]. Since heavy amino acids were used in proliferating myoblasts only, a Heavy to Light (H/L) ratio greater than 2 indicated a significant reduction in protein levels whereas an H/L ratio smaller than 1 indicated an increase in protein levels. Quantitation of total proteome samples from proliferating myoblasts as well as from non-proliferating (differentiated three biologically independent experiments) myocytes were digested with trypsin, and proteins were isolated with LC and an LTQ-Orbitrap Elite mass spectrometer. We identified 4600 proteins of which 4133 were accurately quantitated (Table 1A and Figure 2A). There was good agreement between replicate experiments as indicated by the correlation values (Figure 2B). Of these, 488 proteins were up-regulated and 646 were down-regulated (Table 1) as indicated by H/L ratios higher than 1 (for down-regulated) and lower than 1 (for up-regulated). Notably, we isolated and detected several families of proteins reported to undergo quantitative changes in myoblast differentiation

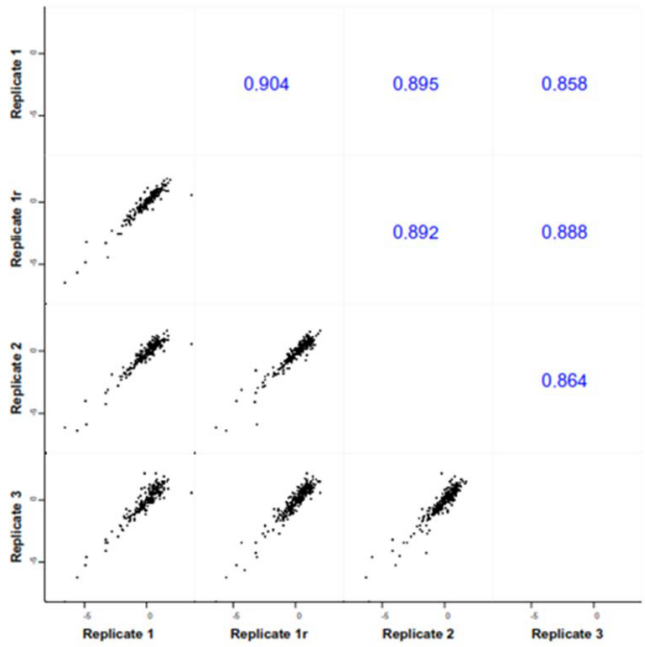

Figure 2B: Correlation values of triplicate experiments.

Group	Number of Proteins
Total	4600
Quantitated	4133
Upregulated	488
Downregulated	646

Table 1a: Number of total proteins iolated by Liquid Chromatography-Mass Spectrometry (LC-MS/MS) from proliferating C2C12 myoblasts and differentiated myocytes, number of prpoteins quantitted and found up- or doenregulated by heavy amino acid SILAC

Number of nodes	136
Number of edges	1848
Average node degree	27.2
Average local clustering coefficient	0.715
Expected number of edges	399
PPI enrichment p-value	$<1.0e^{-16}$

Note: Cytoscape analyzed.

Table 1b: Demethylase network in differentiating mouse C2C12 myoblast cells

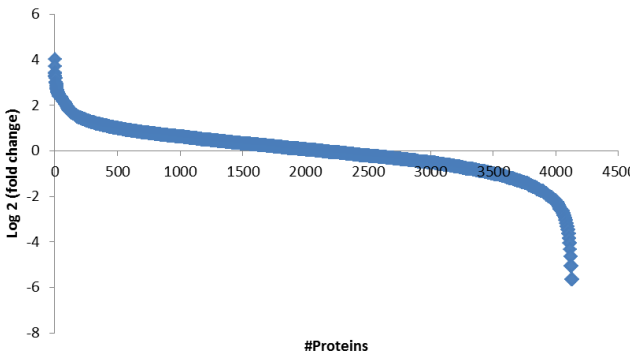

Figure 2A: Log2 ratios of treated vs. control C2C12 cells from heavy SILAC proteomics data (LC-MS/MS) plotted as a function of the number of proteins.

such as RNA-binding proteins and transcription factors (data not shown), confirming our approach [19,20].

As a first step, we examined whether methylation is required for differentiation by treating C2C12 cells with the general methylation inhibitor adenosine dialdehyde (AdOX). AdOX is an inhibitor of S-adenosylhomocysteine hydrolase (AdoHcy hydrolase), and it is useful for studying the role of S-adenosylhomocysteine-regulated processes. AdOX inhibits histone methytransferase (HMTase) activity as well as Arginine methylation. Whereas by day one no effect could be observed with either 5 μM or 50 μM AdOX (Figure 3, lower left panels), there was visible reduction in the per field number of proliferating cells by the third day. The number of proliferating/differentiated cells was reduced even further in the fifth day of treatment with the higher dose having a more pronounced effect (Figure 3, lower right panel). In contrast, control (untreated) cells remained unaffected and had undergone complete differentiation to myocytes by day five (Figure 3, upper panels, C2C123 and 5). These results support the conclusion that global methylation of Arginine on proteins is important for myoblast to myocyte differentiation and open the way for further analysis.

We subjected the protein lists of up- or downregulated genes to Gene Ontology (GO) analysis by extracting enriched pathways during differentiation using analysis with the PANTHER suite of analysis tools (http://pantherdb.org/) and using Fischer's test for statistical overrepresentation (for details see Materials and Methods). The upregulated list was chiefly enriched in genes/proteins active in metabolism such as the respiratory chain, coenzyme metabolism, fatty acid and lipid metabolism and generation of precursor metabolites, reflecting the fact that they are required for differentiating and proliferating myoblasts into quiescent, multinucleated myocytes (Figure 4A). On the other hand, the downregulated list was chiefly enriched in genes/proteins active in the cell cycle as well as in RNA processing, reflecting the fact that during differentiation and after a few

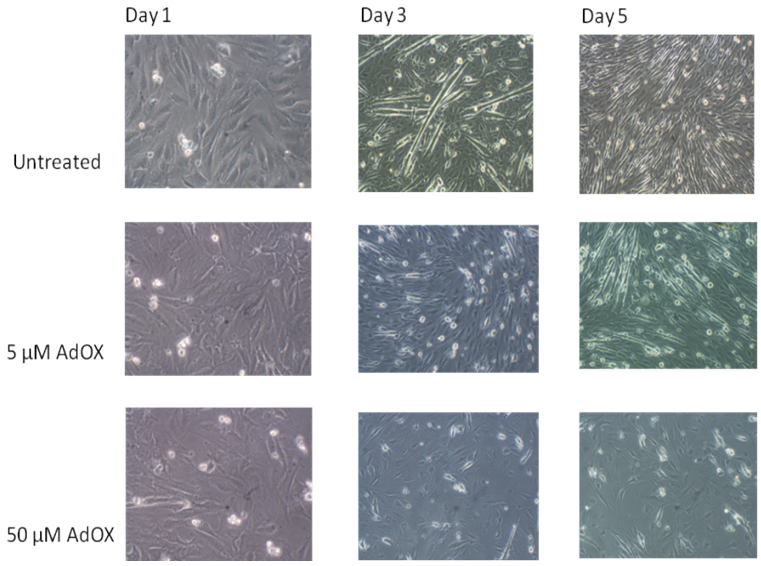

Figure 3: Visible microscopy analysis of C2C12 myoblasts differentiating into myocytes for five days under conditions of reduced (2%) serum (FBS). Untreated (control) cells at days 1, 3 and 5 (upper three panels). Cells treated with 5 µM AdOX at days 1, 3 and 5 (middle panels). 50 µM AdOX added, days 1, 3 and 5 (lower panels). Microscopy was performed with a Nikon microscope equipped with a DXM1200F camera and fields were photographed at 40X or 100X. Shown are 40X images.

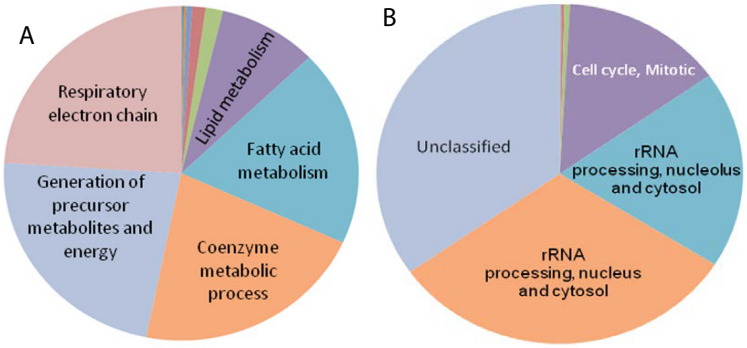

Figure 4: Gene Ontology (GO) analysis data of up- or downregulated proteins from the SILAC proteomics experiments. (A) Top Reactome Pathway GOs for upregulated proteins. (B) Top Reactome Pathway GOs for downregulated proteins. On-web analysis was performed using the PANTHER site as described in Materials and Methods.

divisions, cells stop proliferating and begin the process of expressing genes that are needed for changing their phenotype. Notably, a top enriched group of genes/proteins were unclassified suggesting that they might include members whose functions have not yet been associated with proliferation or differentiation (Figure 4B).

Several Zn-finger proteins, mRNA processing and interacting proteins, a few methylases (two of which are shown in Table 2) and only eight demethylases (Table 2) were among the protein families that are regulated during the transition from proliferating myoblasts to quiescent myocytes. These proteins perform critical functions in chromatin remodeling and in phenotypic switching. The mouse genome is reported to contain forty two (42) demethylase genes encoding eighty seven (87) annotated enzymes (Mouse genome initiative, MGI, http://www.informatics.jax.org/) of which eight underwent quantitative changes between proliferating and differentiated cells (Table 2). Specifically, as indicated by their H/L average ratios from three biologically independent experiments (3.19, 1.99, 1.74 and 1.74 respectively), the levels of the Mina, Jmjd6, Kdm3b, Kdm1a and Kdm5a demethylases were reduced in five-day differentiated myocytes. In contrast, the levels of Phf2 and Cyp51 were modestly up-regulated (H/L ratios equal to 0.77 and 0.55 respectively (Table 2).

We focused on the demethylase enzymes and analyzed the presence of short linear motifs, SLiMs, in their primary sequences using the MEME suite, http://meme-suite.org/db/motifs. It is notable that almost 40% of all proteins contain intrinsically disordered regions, IDRs, and SLiMs within them or are disordered to a great extent. SliMs are important in protein-protein interactions in signaling complexes in almost all cellular processes 23. We identified five novel, statistically significant SLiMs (Figure 5, p-values in panel A and amino acid sequences in panel B), which, on further analysis (data not shown), appeared to be restricted to demethylases. Almost all contain extensive IDRs. We could not retrieve any statistically significant SLiMs for the two methylases and we therefore did not further analyze them, however, given that they are reported for the first time in this model, they merit further scrutiny. Notably, demethylases Kdm7a and Phf2 contain all five identified SliMs suggesting multiple interactions in their complexes (Figure 5, panel B). Interestingly, Kdm7a is known to play a role in brain development. Our report is the first to report Kdm7a regulation in in

Type	Accession	Gene	Protein Description	Proteins	Unique Peptides	Peptides	PSMs	Fold change (Heavy)/ (Light)	Annotated Biochemical Function	Regulation
DEMETHYLASES	XP_006522542	*Mina*	PREDICTED: bifunctional lysine-specific demethylase and histidyl-hydroxylase MINA isoform X1	2	3	3	4	3.19	H3K9me3	Downregulated
	XP_006532023	*Jmjd6*	PREDICTED: bifunctional arginine demethylase and lysyl-hydroxylase JMJD6 isoform X1	2	3	3	4	1.99	H3K9, H3R2, H4R3	Downregulated
	NP_001074725	*Kdm3b*	Lysine-specific demethylase 3B	3	1	1	2	1.94	H3K9	Downregulated
	XP_006539392	*Kdm1a*	PREDICTED: lysine-specific histone demethylase 1A isoform X1	4	4	4	7	1.74	H3K4me2, H3K9	Downregulated
	NP_666109	*Kdm5a*	Lysine-specific demethylase 5A	11	1	1	1	1.74	H3K4me2, H3K4me3	Downregulated
	NP_035208	*Phf2*	Lysine-specific demethylase PHF2	1	1	1	2	0.72	H3K9	Upregulated
	NP_064394	*Cyp51*	lanosterol 14-alpha demethylase	1	9	9	13	0.55	sterol 14-demethylase activity	Upregulated
	NP_001028602	*Kdm7a*	Lysine-specific demethylase 7A	1	1	1	1		H3K27, H3K36, H3K9, H4K20	-
METHYLASES	NP_663379	*Prmt7*	protein arginine N-methyltransferase 7	1	2	2	2	1.75	H4R3me2s	Upregulated
	NP_080780	*Coq5*	2-methoxy-6-polyprenyl-1,4-benzoquinol methylase, mitochondrial precursor	1	2	2	2	0.37	conversion of 2-polyprenyl-6-methoxy-1,4-benzoquinol (DDMQH2) to 2-polyprenyl-3-methyl-6-methoxy-1,4-benzoquinol (DMQH2)	-

Table 2: Methylase and demethylase enzymes discovered by LC-MS/MS proteomics to undergo quantitative level changes in proliferating C2C12 muoblasts and differentiated myocytes, the number of unique peptides and total peptides isolated, the Heavy-to-Light (H/L) changes and the annotated biochemical function of each enzyme. Note that five out of eight demehtylase enzymes demethylate H3K9.

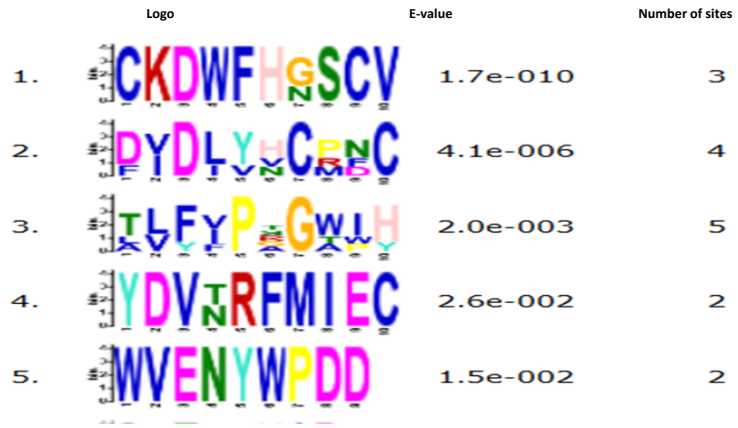

Figure 5(A): Short linear motifs, SliMs, present in demethylases regulated during myoblast differentiation. The top SLiMs in demethylases whose levels are regulated during myoblast differentiation.

vitro muscle differentiation. It demethylates dimethylated Lysine 9 and Lysine 7 (H3K9me2 and H3K27me2, respectively) on histone H3 and monomethylated histone H4 Lysine 20 residue (H4K20Me1). Therefore is appears to be important for the histone code. On the other hand, Phf2 is enzymatically inactive, and becomes activated by PKA-mediated phosphorylation. This leads to complex formation with ARID5B and demethylation of methylated ARID5B. Demethylation of ARID5B causes the PHF2-ARID5B complex to dimethylate Lys-9 on histone H3 (H3K9me2) on target promoters, catalyzing its demethylation and concomitant transcription activation of target genes.

A cursory examination of the annotated biochemical functions of the demethylases (Table 2) revealed that five out of eight, demethylate Lysines 9, 27 and 36 on histone 3 and Lysine 36 on Histone 3 ((H3K9, H3K27 and H3K36) and Lysine 20 (H4K20) on histone 4 14. Interestingly, Cyp51 was an exception to the rule suggesting a key role for sterol demethylation in differentiating myoblast cells. Cyp51

Name	Start aa	p-value	Site
8. sp|Q3UWM4|KDM7A_MOUSE	58	6.54e-15	VNRFMIECDV CKDWFHGSCV GVEEHHAVDI
6. sp|Q9WTU0|PHF2_MOUSE	26	6.54e-15	VTRFMIECDA CKDWFHGSCV GVEEEEAPDI
5. sp|Q3UXZ9|KDM5A_MOUSE	1180	1.73e-14	ASGFMLQCEL CKDWFHNSCV PLPKSSSQKK
6. sp|Q9WTU0|PHF2_MOUSE	44	6.15e-15	CVGVEEEEAP DIDIYHCPNC EKTHGKSTLK
8. sp|Q3UWM4|KDM7A_MOUSE	76	3.18e-14	CVGVEEHHAV DIDLYHCPDC AALHGSSLMK
3. sp|Q6ZPY7|KDM3B_MOUSE	1243	1.69e-11	EAFSQEFGDQ DVDLVNCRNC AIISDVKVRD
5. sp|Q3UXZ9|KDM5A_MOUSE	290	4.33e-10	RQRKGTLSVN FVDLYVCMFC GRGNNEDKLL
8. sp|Q3UWM4|KDM7A_MOUSE	345	1.53e-13	CYKCVVKQGH TLFVPTGWIH AVLTSQDCMA
6. sp|Q9WTU0|PHF2_MOUSE	312	1.47e-12	CYKCTVKQGQ TLFIPSGWIY ATLTPVDCLA
2. sp|Q9ERI5|JMJD6_MOUSE	264	2.63e-12	PLEILQKPGE TVFVPGGWWH VVLNLDTTIA
3. sp|Q6ZPY7|KDM3B_MOUSE	1481	2.40e-9	GWAIVQFLGD AVFIPAGAPH QVHNLYSCIK
1. sp|Q8CD15|RIOX2_MOUSE	231	8.62e-9	THDFLLKPGD LLYFPRGTIH QAETPSGLAY
8. sp|Q3UWM4|KDM7A_MOUSE	46	6.08e-15	PPVYCVCRQP YDVNRFMIEC DVCKDWFHGS
6. sp|Q9WTU0|PHF2_MOUSE	14	1.49e-14	VPVYCVCRLP YDVTRFMIEC DACKDWFHGS
8. sp|Q3UWM4|KDM7A_MOUSE	250	1.53e-13	EVPDIARKLS WVENYWPDD SVFPKPFVQK
6. sp|Q9WTU0|PHF2_MOUSE	217	1.53e-13	EPPDIVKKLS WVENYWPDD ALLAKPKVTK

Figure 5(B): Short linear motifs, SliMs, present in demethylases regulated during myoblast differentiation. Distribution of the top SLiMs in the demethylase enzymes regulated during myoblast differentiation, their amino acid sequences, start amino acid and relative p-values calculated with the MEME algorithm.

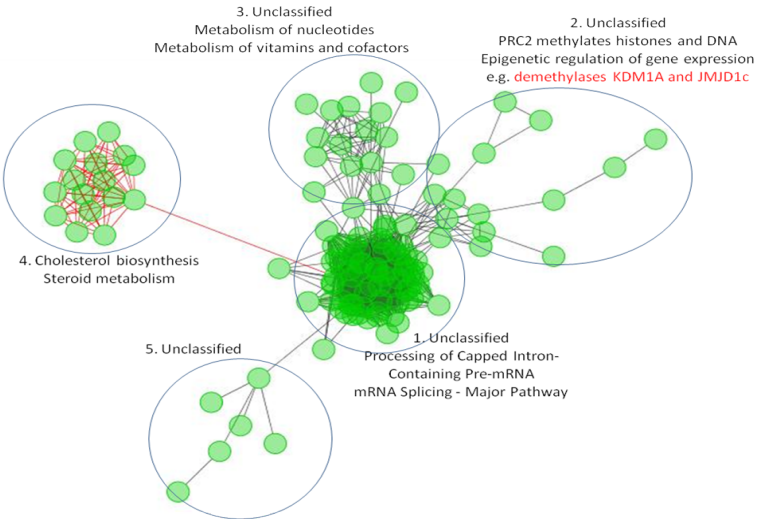

Figure 6(A): Network of eight demethylases in mouse C2C12 myoblasts undergoing differentiation to myocytes, and clustered into five subnetworks. Shown are the Reactome Pathway enriched GOs. Network reconstruction was performed with Cytoscape (https://cytoscape.org/) as described in Materials and Methods.

is involved in step 1 of the pathway that synthesizes zymosterol from lanosterol catalyzing C14-demethylation of lanosterol. Further analysis of the presence of enriched domains revealed the presence (5 out of 8) of the JmdC and JmdN domains. Jumonji demethylase enzymes are known to regulate myogenic differentiation and this was a confirmation of our findings [21-23]. Also, present were the PHD, zf-C5HC2, amino oxidase, SWIRM and Cupin-4 domains. Whereas methylation of H3K4, H3K36 and H3K79 is mainly correlated with transcriptional activation in euchromatin [14,24], methylation of H3K9, H3K27, and H4K20 correlate with transcriptionally silent chromatin (heterochromatin). The presence of demethylases that demethylate Lysines on histone 3 correlates with active and inactive chromatin transcription. This reflects the complexity of modifications that chromatin must undergo, in coordination with other types of post-translational modifications, so that cells execute their differentiation programs. Demethylation of Lysines [9,24] on histone 3 and 20 on histone 4 play a critical role in the above-mentioned processes. Although demethylases are required for differentiation of myoblasts to myocytes [25], it remains an open question how their activities are integrated with the differentiation machinery. One mechanism is probably via interactions with transcription factors [26-28].

In order to place the demethylases in the context of a C2C12 cell differentiation network, we employed them as queries and extracted their interactions from the STRING database. We then employed the Cytoscape program and reconstructed a network containing 137 nodes and over 1800 edges (Materials and Methods and Table 1b). Clustering based on top nodes separated the network into 5 distinct sub-networks (clusters) shown in Figure 6A. GO analysis of the clusters revealed that RNA processing proteins are enriched in the top enriched group 1 (Figure 6A), consistent with their importance in differentiation. Group 2 (upper right, Figure 6A) is enriched in proteins participating in epigenetic regulation of gene expression and also in demethylases KDM1a and the Jumanji family. Notably, the other groups contain proteins enriched for metabolism and all but

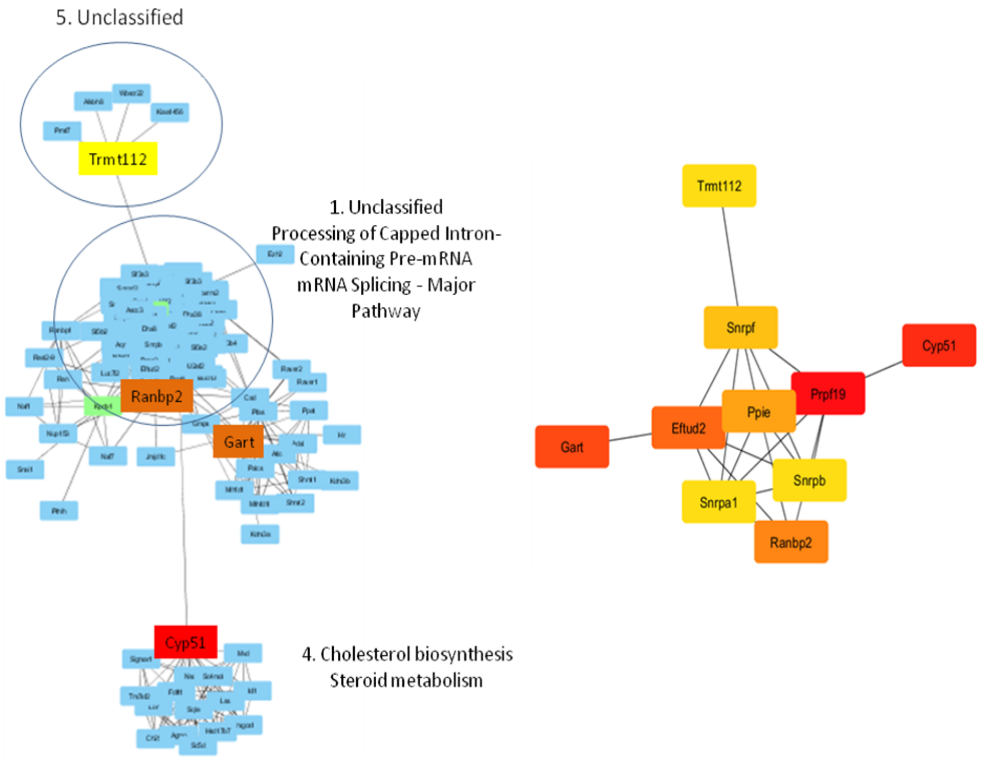

Figure 6(B): Left panel: Demethylase network reorganized to reveal the computed top bottlenecks, distributed in the GO groups in (A). Right panel: Computed shortest paths between top bottlenecks shown in left panel, which include one methylase (Trmt112) and one demethylase (Cyp51).

group 4 are enriched in Reactome pathway proteins not classified by GO. Several methylases and demethylases are distributed in the groups suggesting that their activities might play a role during differentiation. In order to reveal their links, establish their importance and find out if any demethylases or methylases are included, we further analyzed network properties by computing the ten top bottlenecks in the network with the cytoHubba algorithm within Cytoscape. Bottlenecks are important in regulating the stability of networks since they tend to link clusters and therefore to communicate signals of subnetwork functions. As shown in Figure 6B, the top bottleneck proteins in the network are distributed in almost all clusters suggesting that they may have crucial functional roles. Specifically, in cluster 5, we uncovered the Trmt112 Methyltransferase Subunit 11-2, which methylates tRNAs, the Cyp51 lanosterol 14-alpha demethylase, in cluster 4, and in cluster 3, the Gart phosphoribosylglycinamide formyltransferase, phosphoribosylglycinamide and phosphoribosylaminoimidazole synthetase which is involved in de novo purine biosynthesis. We computed the shortest paths between them in order to establish their links. As can be seen in the right panel of Figure 6B, all bottlenecks are three edges apart (shortest path equal to 3) suggesting that they may be functionally linked. Interestingly, the Eftud2 protein is a GTPase which is a component of the spliceosome complex which processes precursor mRNAs to produce mature mRNAs. Notably, all clusters contain proteins involved in pre-mRNA expression and processing, suggesting that they are critical for gene expression in differentiation.

Conclusion

Our study is one of the first to uncover significant changes in the levels of demethylase enzymes on a proteome-wide level that are regulated in myoblasts differentiating into myocytes. To our knowledge, it is also the first to report the presence of unique SliMs on these demethylase sequences.

Conflict of Interest

The authors declare no conflict of interest.

Acknowledgements

The corresponding author gratefully acknowledges support by a 2014-2015 Hopkins-Libra Fellowship by the Libra Foundation hosted by the Laboratory of Professor Akhilesh Pandey, Department of Biological Chemistry, Johns Hopkins University, Baltimore MD, USA. The corresponding author is particularly grateful to Dr. Min-Sik Kim, Assistant Professor at the Department of Applied Chemistry, Kyung Hee University, Republic of Korea for advice and valuable suggestions on SILAC proteomics, and to Dr. Ahmad Sartaj for support on LC- MS/MS analysis.

References

1. Blais A (2015) Myogenesis in the genomics era. J Mol Biol 427: 2023-2038.
2. Louie KW, Saera-Vila A, Kish PE, Colacino JA, Kahana A (2017) Temporally distinct transcriptional regulation of myocyte dedifferentiation and Myofiber growth during muscle regeneration. BMC Genomics 18: 854.
3. Gong W, Koyano-Nakagawa N, Li T, Garry DJ (2015) Inferring dynamic gene regulatory networks in cardiac differentiation through the integration of multi-dimensional data. BMC Bioinformatics 16: 74.
4. Hernández-Hernández JM, García-González EG, Brun CE, Rudnicki, MA (2017) The myogenic regulatory factors, determinants of muscle development, cell identity and regeneration. Semin Cell Dev Biol 72: 10-18.
5. Khanjyan MV, Yang J, Kayali R, Caldwell T, Bertoni C (2013) A high-content, high-throughput siRNA screen identifies cyclin D2 as a potent regulator of muscle progenitor cell fusion and a target to enhance muscle regeneration. Hum Mol Genet 22: 3283-3295.
6. Gu W, Schneider JW, Condorelli G, Kaushal S, Mahdavi V, et al. (1993) Interaction of myogenic factors and the retinoblastoma protein mediates muscle cell commitment and differentiation. Cell 72: 309-324.

7. Braun T, Gautel M (2011) Transcriptional mechanisms regulating skeletal muscle differentiation, growth and homeostasis. Nat Rev Mol Cell Biol 12: 349-361.

8. Nofziger D, Miyamoto A, Lyons KM, Weinmaster G (1999) Notch signaling imposes two distinct blocks in the differentiation of C2C12 myoblasts. Development 126: 1689-1702.

9. Shawber C, Nofziger D, Hsieh JJ, Lindsell C, Bögler O, et al. (1996) Notch signaling inhibits muscle cell differentiation through a CBF1-independent pathway. Development 122: 3765-3773.

10. Kataoka Y, Matsumura I, Ezoe S, Nakata S, Takigawa E, et al. (2003) Reciprocal inhibition between MyoD and STAT3 in the regulation of growth and differentiation of myoblasts. J Biol Chem 278: 44178-44187.

11. Higashihori, N (2005) Regulation of p21(WAF1/CiP1) expression during cellular differentiation. Kokubyo Gakkai Zasshi 72: 42-48.

12. Shen X, Collier JM, Hlaing M, Zhang L, Delshad EH, et al. (2003) Genome-wide examination of myoblast cell cycle withdrawal during differentiation. Dev Dyn 226: 128-138.

13. Lechner C, Zahalka MA, Giot JF, Møller NP, Ullrich A (1996) ERK6, a mitogen-activated protein kinase involved in C2C12 myoblast differentiation. Proc Natl Acad Sci U.S.A. 93: 4355-4359.

14. Jin W, Peng J, Jiang S (2016) The epigenetic regulation of embryonic myogenesis and adult muscle regeneration by histone methylation modification. Biochem Biophys Rep 6: 209-219.

15. Ong SE, Blagoev B, Kratchmarova I, Kristensen DB, Steen H, et al. (2002) Stable isotope labeling by amino acids in cell culture, SILAC, as a simple and accurate approach to expression proteomics. Mol Cell Proteomics 1: 376-386.

16. Amanchy R, Kalume DE, Pandey A (2005) Stable isotope labeling with amino acids in cell culture (SILAC) for studying dynamics of protein abundance and posttranslational modifications. Sci STKE 2005: 12 .

17. Singh K, Dilworth FJ (2013) Differential modulation of cell cycle progression distinguishes members of the myogenic regulatory factor family of transcription factors. FEBS J 280: 3991-4003.

18. Harada A, Ohkawa Y, Imbalzano AN (2017) Temporal regulation of chromatin during myoblast differentiation. Semin Cell Dev Biol 72: 77-86.

19. Grifone R, Xie X, Bourgeois A, Saquet A, Duprez D, et al. (2014) The RNA-binding protein Rbm24 is transiently expressed in myoblasts and is required for myogenic differentiation during vertebrate development. Mech Dev 134: 1-15.

20. Ravel-Chapuis A, Crawford TE, Blais-Crépeau ML, Bélanger G, Richer CT, et al. (2014) The RNA-binding protein Staufen1 impairs myogenic differentiation via a c-myc-dependent mechanism. Mol Biol Cell 25: 3765-3778.

21. Jung ES, Sim YJ, Jeong HS, Kim SJ, Yun YJ, et al. (2015) Jmjd2C increases MyoD transcriptional activity through inhibiting G9a-dependent MyoD degradation. Biochim Biophys Acta 1849: 1081-1094.

22. Bodega B, Ramirez GDC, Grasser F, Cheli S, Brunelli S, et al. (2009) Remodeling of the chromatin structure of the facioscapulohumeral muscular dystrophy (FSHD) locus and upregulation of FSHD-related gene 1 (FRG1) expression during human myogenic differentiation. BMC Biol 7: 41.

23. Luo D, de Morree A, Boutet S, Quach N, Natu V, et al. (2017) Deltex2 represses MyoD expression and inhibits myogenic differentiation by acting as a negative regulator of Jmjd1c. Proc Natl Acad Sci U.S.A. 114: E3071-E3080.

24. Kimura H (2013) Histone modifications for human epigenome analysis. J Hum Genet 58: 439-445.

25. Benevolenskaya EV (2007) Histone H3K4 demethylases are essential in development and differentiation. Biochem Cell Biol 85: 435-443.

26. Choi J, Jang H, Kim H, Kim ST, Cho EJ, et al. (2010) Histone demethylase LSD1 is required to induce skeletal muscle differentiation by regulating myogenic factors. Biochem Biophys Res Commun 401: 327-332.

27. Choi JH, Song YJ, Lee H (2015) The histone demethylase KDM4B interacts with MyoD to regulate myogenic differentiation in C2C12 myoblast cells. Biochem Biophys Res Commun 456: 872-878.

28. Verrier L, Escaffit F, Chailleux C, Trouche D, Vandromme M (2011) A new isoform of the histone demethylase JMJD2A/KDM4A is required for skeletal muscle differentiation. PLoS Genet 7: e1001390.